Spring 2018

Investigating the Relationship Between Sulcogyral Patterns and Structural and Functional Connectivity Metrics in the Orbitofrontal Cortex

Bethany M. Blass
Bucknell University, bmb030@bucknell.edu

INVESTIGATING THE RELATIONSHIP BETWEEN SULCOGYRAL PATTERNS AND STRUCTURAL AND FUNCTIONAL CONNECTIVITY METRICS IN THE ORBITOFRONTAL CORTEX

by

Bethany M. Blass

A Thesis Submitted to the Honors Council
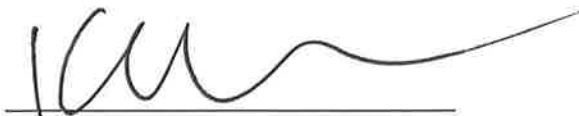For Honors in Neuroscience

Approved by:

_____
Advisor: Judith Grisel

_____
Co-Advisor: Vanessa Troiani

_____
Department Chairperson: Kevin Myers

Table of Contents

List of Tables:

List of Figures:

1. Abstract

Located within the frontal lobe, the human orbitofrontal cortex (OFC) is widely known for its roles in sensory integration, emotion processing, decision-making, and goal-directed behaviors. Atypical structural organization of the OFC may explain atypical social or motivational behaviors displayed by individuals with brain disorders, such as bipolar disorder patients (BP).

The human brain can be imaged using magnetic resonance imaging (MRI) to reveal interesting aspects of the underlying brain architecture. This brain is composed of different tissue types, including gray and white matter, as well as various morphological features, including sulci & gyri. Within the OFC, the sulci can be labeled and classified into a finite number of patterns based on the continuity of the most medial and most lateral sulci. Typical patterns (Type I) have previously been found at higher frequencies bilaterally in healthy populations, whereas atypical patterns (Type II and Type III) have been found at higher frequencies in relative to patients with schizophrenia (SZ).

In order to characterize differences in morphological properties of structural OFC architecture in BP patients (N=46) relative to healthy controls (N=52), we trace OFC sulcogyral patterns based on a previously established protocol, employ a voxel-based morphometry (VBM) analysis to assess OFC gray matter (GM), and implement a diffusion tensor imaging (DTI) tractography analysis to measure white matter tract microstructural properties. Chi-square analysis compared sulcogyral pattern frequency distributions between groups, and independent sample t-tests compared additional OFC

properties. Based on previous work and overlap of symptoms and genetics between BP and SZ, we predict that OFC architecture in BP individuals will differ from controls.

We find that BP displayed increased atypical (Type II and Type III) sulcal pattern frequencies relative to controls in the left hemisphere ($\chi^2 = 18.6$, $p < 0.001$). T-tests reveal that global OFC GM volumes were significantly decreased in both right ($p = 0.0338$) and left ($p = 0.0039$) hemispheres of BP relative to controls. BP also exhibit a reduced number of tracts in the uncinate fasciculus (UF) relative to controls on the left that trended toward significance ($p = 0.094$).

Overall, we find atypical OFC structural organization of sulcal patterns, reduced gray matter volume, and fewer white matter UF tracts in BP relative to controls, especially in the left hemisphere. Exploring and quantifying various structural brain properties within the OFC may be useful in assessing individual risk to brain dysfunction and facilitate a personalized approach for diagnosis and treatment.

2. Introduction and Background

The orbitofrontal cortex (OFC) is a region of the prefrontal cortex situated in the frontal lobe of the brain, and is located on the ventral surface of the frontal region. The OFC has been implicated in personality or behavior for over a century, with more recent theoretical work suggesting roles in sensory integration, emotion processing, expectation, motivation, decision-making, and goal-directed behaviors (Murray, O'Doherty, & Schoenbaum, 2007; Kringelbach, 2005). The OFC is highly connected to multiple brain regions, including the hypothalamus, amygdala, insula, medial prefrontal cortex, and the basal ganglia (Kringelbach, 2005). The OFC also displays considerable individual variability (Chiavaras & Petrides, 2000; Kringelbach, 2005), which can make it challenging to understand its role in normal human behavior. Investigating variability and abnormal structural organization of the OFC may explain atypical behaviors displayed by individuals with various psychiatric disorders (Jackowski et al., 2012).

Bipolar disorder (BP) is a classification of affective disorders in which patients experience episodes of mania or depression, irritable or elated moods, or hypomania. There are several subtypes of bipolar disorder, including Bipolar I, Bipolar II, Cyclothymia, and Bipolar, unspecified. We focus here on Bipolar disorder I, which is characterized by episodes of depression and at least one incident of full-blown mania (American Psychiatric Association, 2013; Phillips & Kupfer, 2013). Previous research has examined OFC structural variability extensively in disorders such as schizophrenia (SZ) (Bartholomeusz et al., 2013; Chakirova et al., 2010; Chiavaras & Petrides, 2000;

Lavoie et al., 2014; Takayanagi et al., 2010), but recently, OFC sulcal variability has been investigated in BP (Patti & Troiani, 2018). Due to the overlap in behavioral and genetic etiology of SZ and BP and previous research implicating atypical OFC variability in BP, we choose to investigate OFC structural properties of patients with BP.

The overall goal of this thesis is to characterize differences in multiple morphological properties of the OFC in BP and otherwise healthy controls. We focus on three different types of brain metrics and analyses, each described in detail below. Further, we describe existing knowledge using each of these analysis methods in patients with BP and separately, patients with SZ. Although we did not analyze data from SZ patients as part of this thesis work, knowledge on the background of both disorders is relevant to interpretation and future directions.

2.1 Orbitofrontal Sulcogyral Patterns

Within the OFC, an H-shaped sulcus is formed by the intersection of the medial orbital sulcus (MOS), lateral orbital sulcus (LOS), and transverse orbital sulcus (TOS). The distinct pattern formed by these sulci varies between individuals and can be categorized into one of three identified arrangements (Type I, Type II, Type III) by manually tracing the sulci (Chiavaras & Petrides, 2000). Sulcogyral patterns can be used as a basis for structural analysis of the internal surface anatomy, as they distinguish functionally distinct brain regions and provide a natural topography of the brain's

anatomy. Within the human cerebral cortex, sulcal landmarks can be identified via magnetic resonance images (MRI) to classify sulcogyral patterns.

Type I is the most common pattern identified in typical populations of humans and monkeys (Chiavaras & Petrides, 2000). Type II and Type III patterns have been found at higher frequencies in patients with SZ relative to controls (Bartholomeusz et al., 2013; Chakirova et al., 2010; Lavoie et al., 2014; Takayanagi et al., 2010) and are thought to indicate atypical OFC organization. The association of Type I with typical phenotype suggests that the Type I pattern may serve as a protective buffer against the development of disorders such as SZ. Our lab has recently identified atypical OFC sulcogyral patterns in patients with bipolar disorder I (BP I) and attention deficit disorder (ADHD), which suggests that sulcogyral patterns may present a morphological indicator for increased susceptibility to multiple psychiatric diagnoses (Patti & Troiani, 2018). It is unknown whether other gray and white matter volumetric differences are present in the OFC of individuals with BP.

An aim of this study is to characterize structural properties such as orbitofrontal sulcogyral patterns in BP and controls. We expect that due to the similarity of clinical symptoms and behaviors associated with BP relative to SZ, the frequencies of sulcogyral pattern types will be consistent with previous findings in SZ (Carroll & Owen, 2009; Chiavaras & Petrides, 2000). That is, we expect that control subjects will exhibit the highest frequencies of Type I sulcogyral pattern bilaterally, and we hypothesize BP will display higher frequencies of atypical patterns (Type II and Type III) relative to controls.

In addition, this study will explore gray matter and white matter differences in the OFC between these groups.

2.2 Gray Matter Volume

In addition to variability among OFC sulcogyral patterns described above, individual differences in gray matter (GM) volume in the brain can be measured to further quantify structural brain architecture. One of the most common methods of assessing GM differences is voxel-based morphometry (VBM) (Ashburner & Friston, 2000; Good et al., 2001; Kanai & Rees, 2011). VBM preprocessing results in the segmentation of anatomical MRI images into gray matter, white matter, and cerebrospinal fluid tissue types. Each subject's image is then spatially warped into a common stereotactic space, and smoothed. Processed images then represent local volumes of the selected tissue type (gray matter, white matter, etc.) at individual voxels, and differences between groups can be assessed using statistical analyses. These statistical maps can also be used to investigate relationships between brain volume metrics and behavior in the form of correlations (Kanai & Rees, 2011).

Structural brain imaging has demonstrated that SZ patients exhibit abnormalities in GM relative to controls. In patients with SZ, the H-shaped sulcus has been linked to brain volume reduction (Nakamura et al., 2007a). Studies investigating the relationship between OFC volumetric differences between healthy controls and SZ patients have suggested that reductions in total subregional OFC volumes are typical in chronic SZ (Nakamura et al., 2007b; Takayanagi et al., 2010). Several studies have identified GM

volume reductions in cortical and subcortical regions of SZ patients, shown in region of interest (ROI) analyses (Wright et al., 2000) and VBM analyses (Job et al., 2002; Kubicki et al., 2002). VBM analysis of SZ patients also revealed reduced GM volume in anterior thalamus, middle prefrontal gyrus, and dorsomedial thalamus relative to control subjects (McIntosh et al., 2005). Additionally, progressive GM reductions in the OFC are common from the initial onset of the illness (Bora, Fornito, Pantelis, & Yücel, 2012).

Though GM findings regarding SZ are robust and consistently replicated, the structural brain abnormalities underlying BP are less well known. It has been suggested that emotional, behavioral, and cognitive deficits manifested in BP are due to a disruption in the neurocircuitry of the OFC, which extends to the amygdala, striatum, thalamus, and hypothalamus (Monkul, Malhi, & Soares, 2005; Nery et al., 2009; Strakowski, Delbello, & Adler, 2005). However, GM volume differences in BP populations are inconsistent and less robust. For example, a voxel-by-voxel automated analysis one study demonstrated reduced bilateral OFC GM volumes compared to BP I patients (Frangou, Donaldson, Hadjulis, Landau, & Goldstein, 2005). However, a VBM analysis found decreased GM volumes in the left hemispheres of medicated bipolar I and II patients relative to controls, but no differences were found in medication-free BP patients relative to controls (Nugent et al., 2006). In a study by Nery et al. (2009) that used manual tracings of the OFC to derive regions of interest, there were no differences found in GM volumes of total OFC or its subdivisions between controls and mixed BP patients (BP I and BP II). Thus, it could be that OFC GM volumes do not represent a general characteristic of BP, but may be linked to specific clinical features of the disorder (Nery et al., 2009).

A second aim of our study is to further characterize structural OFC properties in BP to add to the growing body of literature on this topic. We will employ an automated VBM analysis to quantify GM volumes in total OFC and OFC sub-regions in BP and controls. We expect that BP patients will display reduced OFC GM volumes relative to controls.

2.3 White Matter/Uncinate Fasciculus

In addition to gray matter structural properties, white matter (WM) microstructural properties can be estimated in the human brain (Fields, 2008; Johansen-Berg, 2010). Diffusion tensor imaging (DTI) provides a technique to determine WM integrity and neuronal connectivity within the brain by employing diffusion-weighted magnetic resonance imaging (DW-MRI) to quantify the diffusion of water molecules across brain tissue (Skudlarski et al., 2008). DW-MRI provides a quantification of WM structural properties, including the degree of water diffusion that results from tissue boundaries such as cell membranes across individual voxels within the brain (Alm, Rolheiser, Mohamed, & Olson, 2015). Several metrics can be quantified using DW-MRI, including fractional anisotropy (FA) and deterministic tractography. FA is an average measure of regional WM features, with higher FA values indicating more efficient neuronal conduction via WM tracts (Alexander, Lee, Lazar, & Field, 2007; Beaulieu, 2002). Deterministic tractography methods are a way of visualizing specific white matter tracts and estimate the strength of a connection between two selected ROIs. Thus,

estimates of tract connectivity in individuals might explain inter-individual differences in behavior (Kanai & Rees, 2011).

The disconnection hypothesis of SZ suggests that the disorder is a result of atypical connectivity between the prefrontal cortex and structures such as the thalamus, striatum, or temporal lobe (Friston & Frith, 1995; McIntosh et al., 2008). Findings from DTI studies have consistently supported the hypothesis, revealing that WM density is reduced in SZ patients (Buchsbaum et al., 2006; Burns et al., 2003), and deficits specific to the uncinate fasciculus (UF) are present by the first psychotic episode (Price et al., 2008). The UF is a hook-shaped bundle of WM tracts that connects limbic system regions of the OFC, and abnormalities within the UF have been associated with social anxiety and depression. Findings supporting the disconnection hypothesis of SZ have also extended to bipolar disorder (McIntosh et al., 2008).

Evidence exists of WM abnormalities and altered connectivity in BP. Prior work has suggested that WM is reduced in BP I patients relative to controls (Adler et al., 2004; Regenold et al., 2006; McIntosh et al., 2005). Additionally, BP I and SZ patients had reduced FA in the anterior limb of the internal capsule (ALIC), anterior thalamic radiation (ATR), and in the UF relative to controls (Sussmann et al., 2009). Reductions in the UF and ATR were also found in patients with SZ and BP relative to controls (McIntosh et al., 2008).

Our DTI analysis yields a three-dimensional reconstruction of WM tracts within the brain of each subject. Because of the limited findings implicating UF deficits in BP, we choose to isolate the UF. Isolating tracts of the UF rather than all tracts within the

OFC allows us to more precisely reveal its structural connectivity profile, and focus on a well-known tract of fibers connecting the OFC to additional brain regions. Thus, a third aim of this project is to extract several metrics of WM microstructural properties of bilateral UF to quantify WM properties of BP relative to controls. We expect that the mean FA values and number of tracts within the UF of BP subjects will be atypical relative to control subjects.

Overall, we are interested in investigating structural brain architecture of BP I patients to better understand phenotypic manifestations and biological markers specific to the disorder. Additionally, we are interested in exploring whether OFC sulcogyral pattern type influences structural connectivity as measured by several other brain analysis metrics. Inter-individual differences in regional brain structure frequently co-vary with inter-individual differences in functionally connected brain regions, known as structural co-variance (Alexander-Bloch, Giedd, & Bullmore, 2013). Employing VBM and DTI tractography analyses will allow us to examine how structural properties of the H-shaped sulcus within the OFC correspond to connectivity in BP.

3. Materials and Methods

3.1 Ethics Statement

The research protocol and consent procedures were approved by the Institutional Review Boards at the University of California Los Angeles (UCLA) and the Los Angeles County Department of Mental Health. All subjects provided written and informed consent.

3.2 Participants

Structural images were acquired from the OpenfMRI database (accession number ds000030), a publically accessible and anonymized data set made available by the University of California Los Angeles Consortium for Neuropsychiatric Phenomics and can be obtained at: https://openfmri.org/dataset/ds000030/. Participants included right-handed English- or Spanish-speaking controls, and patients with self-reported bipolar disorder. Patients were assessed with the Structured Clinical Interview for DSM Disorders (SCID-IV) (First, Spitzer, Gibbon, & Williams, 1995) to verify history and/or absence of psychopathology and a urine drug screen to assess drug use. (See Tables 1a and 1b for demographic information). Bipolar patients were recruited using a patient-oriented strategy involving outreach to local clinics and online portals, while controls were recruited using advertisements in Los Angeles area newspapers. All candidates were

screened via telephone and in person. Additional information about this cohort can be

found at:

https://web.archive.org/web/20151229081105/http://www.phenowiki.org/wiki/index.php/

LA5C

Control subjects from the larger cohort were only included if they had no Axis I

diagnosis, as confirmed by the SCID-IV (N=56). In addition, only bipolar patients with a

confirmed diagnosis for Bipolar I Disorder using the SCID-IV were included (N=49).

Although the publically accessible data set already excluded participants with

excessive motion, we additionally excluded several subjects (N=7) whose motion caused

noise in the orbitofrontal cortex region of the structural image, thus restricting the ability

to make accurate sulcal tracing classifications (BP N=3, Control N=4). Thus, the cohort

was reduced to N=98 (BP N=46, Control N=52). Table 1a includes demographic

information regarding subjects used in the analyses regarding sulcogyral pattern

classification and the voxel-based morphometry gray matter analysis.

Table 1a. **Demographic characteristics of all subjects.**

	Male:Female		Scanner Site 1: Scanner Site 2		Age (years) Mean ± SD	Education (years) Mean ± SD
HC *(N=52)*	N	23:29	N	42:10	30.8 ± 8.9	15.0 ± 1.7
	%	44:56	%	81:19		
BP *(N=46)*	N	27:19	N	25:21	35.3 ± 9.3	14.5 ± 1.9
	%	59:41	%	54:46		
HC vs. BP χ^2 / F / t *(p)*	2.04 (*p*=0.153)		7.88 (*p*=0.005)		-2.47 (*p*=0.015)	1.36 (*p*=0.179)

HC = healthy controls; BP = bipolar

During the next analysis in which images were put through our DTI pipeline, additional participants were excluded (N=15; BP N=5, Control N=10) due to failing quality control checks. Participants were excluded if they were missing diffusion weighted image data (i.e. the sequence was not run at all) or due to the angle of acquisition removing the temporal lobe out of frame of the image, which limited the ability to complete DTI analysis. The final subgroup used for DTI analysis was reduced to N=83 (BP N=41, Control N=42). Table 1b includes demographic information regarding subjects used in the DTI analysis.

Table 1b. Demographic characteristics of subgroup included in DTI analysis.

		Male:Female		Scanner Site 1: Scanner Site 2	Age (years) Mean ± SD	Education (years) Mean ± SD
HC *(N=42)*	N	20:22	N	32:10	30.6 ± 9.0	14.9 ± 1.8
	%	48:52	%	76:24		
BP *(N=41)*	N	25:16	N	22:19	35.4 ± 9.4	14.4 ± 1.9
	%	61:39	%	51:49		
HC vs. BP χ^2 / F / t *(p)*		1.49 (*p*=0.222)		4.63 (*p*=0.031)	-2.39 (*p*=0.019)	1.09 (*p*=0.279)

HC = healthy controls; BP = bipolar

3.3 Demographics and Phenotype Characterization

3.3.1 Demographics

The study link above contains a complete list of all phenotype variables, some of which were acquired in the entire cohort and others in specific patient samples. Relevant to the current study, age, gender, education level, and clinician-interview instruments pertinent to the phenotype of bipolar patients are reported.

3.3.2 Phenotype Characterization

Phenotype metrics commonly used to assess psychiatric-disorder specific groups are also included to further describe the behavioral phenotype of the subjects. Since the majority of clinician-interview instruments were not ascertained on the control subjects, several self-report questionnaires that evaluate similar psychometric domains are included. These metrics and the purpose for describing them in this analysis are reported below, and averages for the subject groups are reported in Table 2.

Table 2. Phenotypic characteristics. Columns on the left include phenotype information on all subjects, and columns to the right are specific to the subgroup of subjects included in DTI analysis. (YMRS = Young Mania Rating Scale; HPS = Hypomanic Personality Scale; BPII = Bipolar II Summary Score).

| | All Subjects | | | | | DTI Subgroup | | | | |
| | HC (N=52) | | BP (N=46) | | HC vs. BP t (p) | HC (N=42) | | BP (N=41) | | HC vs. BP t (p) |
	Mean	SD	Mean	SD		Mean	SD	Mean	SD	
YMRS	--	--	12.4	11.2	--	--	--	12.6	11.4	--
HPS	16.2	7.6	24.8	11.1	-4.51 (p<0.001)	15.6	6.6	24.4	11.5	-4.29 (p<0.001)
BPII	11.1	4.7	17.2	6.5	-5.37 (p<0.001)	10.6	4.5	16.8	6.7	-4.92 (p<0.001)

HC = healthy controls; BP = bipolar

3.3.2.1 Clinician Interview Instruments

The Structured Clinical Interview for DSM-IV Axis I Disorders (SCID-IV) (First et al., 1995) is a clinician-administered assessment used to diagnose DSM-IV Axis I mental disorders. All participants were administered this interview. Controls were determined based on the confirmation of "No Axis I Diagnosis" and all bipolar patients included in this analysis had a confirmed diagnosis of bipolar disorder I.

Young Mania Rating Scale (YMRS) (Young, Biggs, Ziegler, & Meyer, 1978) is an 11-item clinician-administered instrument that was created to evaluate the severity of manic episodes in patients with bipolar disorder. Scores range from 0-60 with a cutoff score of >20 indicating the presence of manic symptoms. Only bipolar patients were administered this assessment.

3.3.2.2 Self-Report Instruments

The Hypomanic Personality Scale (HPS) (Eckblad & Chapman, 1986) is a Chapman Scale developed to evaluate the overactive, sociable personality style associated with episodes of hypomanic euphoria associated with bipolar disorder. This self-report assessment consists of 48 True-False items, scores ranging from 0 to 48, with higher scores indicating the presence of more features associated with a hypomanic personality. This scale is included to demonstrate the differences in mania symptoms between patient and control subjects.

3.4 Neuroimaging

3.4.1 Image Acquisition

Magnetic Resonance Imaging (MRI) scanning was conducted at two different locations, Ahmanson-Lovelace Brain Mapping Center and the Staglin Center for Cognitive Neuroscience, on a 3T Siemens Trio scanner. High-resolution anatomical images (T_1-weighted 3D MPRAGE) were collected for each participant with the following parameters: 1 mm^3 voxel size, 176 axial slices, 1 mm slice thickness, TR = 1.9 s, TE = 2.26 ms, FOV = 250, matrix = 256 X 256 sagittal plane. As detailed above, additional participants were excluded due to excessive motion, which caused noise in the OFC region of the structural image. Control subjects were mostly collected on one scanner, while the bipolar patient group was roughly split between the two scanners (see Table 1a). Regardless of the scanner location, the same sequence was used for all subjects. Recent work has confirmed that sulcal pattern characterization is a robust measure that is not influenced by the scanner site (Chye et al., 2017). Thus, it is unlikely that structural properties such as sulcal pattern type, GM volume, or WM tracts would be influenced by scanner site.

3.4.2 Preprocessing

Anatomical images were normalized by stripping non-brain tissue using FMRIB

Software Library (FSL) Brain Extraction Tool (BET) (Smith, 2002), then aligned along

the anterior commissure-posterior commissure (AC-PC) plane to adjust for head tilt

(using FMRIB Linear Image Registration Tool, FLIRT) (Jenkinson, Bannister, Brady, &

Smith, 2002; Jenkinson & Smith, 2001) after registration to an MNI template, and

resampled into 1mm cubic voxels (Greve & Fischl, 2009). The fractional intensity

threshold in BET was set to 0.3, which sometimes resulted in residual skull or brainstem

being left in the image but assured that portions of the brain surface were not

unintentionally removed.

3.4.3 Sulcal Pattern Tracing

The OFC sulcal patterns were identified from the normalized images and

classified according to the criteria used in previous characterizations of OFC sulcal

patterns (Lavoie et al., 2014). OFC sulcal patterns were previously classified in the OFC

of each hemisphere by three tracers (including author of this thesis, B.B.) blinded to

subject diagnosis using ITK-SNAP, a digital software application which segments

structures in 3D medical images (Patti & Troiani, 2018; Yushkevich et al., 2006).

Following previously published methods, anatomical landmarks serving as boundaries for

OFC subregions were manually referenced. The appropriate sulcal regions were

identified according to an explicit tracing and classification procedure, and then manually

traced. Once OFC sulci were identified and traced, the OFC sulcogyral pattern type was objectively determined in each hemisphere using a previously established classification rubric (Patti & Troiani, 2018) defined by Chiavaras and Petrides (2000) and adapted by Bartholomeusz et al., (2013), which consists of Type I, II, and III/IV patterns based on the continuity of the medial and lateral orbital sulci. (All 98 subjects included in this analysis; see Table 1a for details).

Type I consists of a discontinuous medial orbital sulcus (MOS) and continuous lateral orbital sulcus (LOS), Type II a continuous MOS and LOS, and Type III a discontinuous MOS and discontinuous LOS (see Figure 1). Comparable to previous studies, all subjects with an H-sulcus pattern classified by the rare Type IV pattern (continuous MOS and discontinuous LOS) were included with Type III patterns for analyses (Bartholomeusz et al., 2013). Each subject's bilateral OFC sulcal pattern was independently traced and classified by three trained tracers (M.P., B.B., & R.V.), including the author of this thesis (B.B.), blinded to diagnosis. A subset of 20 randomly selected brains (40 hemispheres) were also reviewed by V.T. to confirm classification validity. Interrater reliability between tracers and V.T. was very good (K = 0.863 (95% CI, 0.726 to 1), p<0.0005). M.P. then re-characterized a subset of brains in order to obtain an interrater reliability statistic. Interrater reliability was also very good (K = 0.909 (95% CI, 0.787 to 1), p<0.0005).
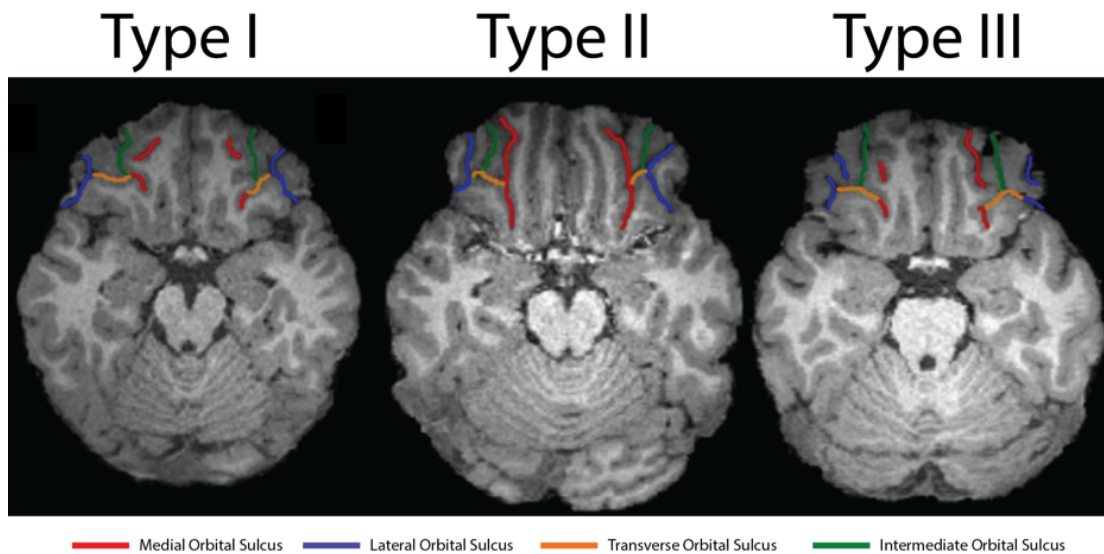
Figure 1. Examples of different H-sulcus pattern types in sample axial images. Type I, on the far left, is characterized by a discontinuous Medial Orbital Sulcus (MOS, in red) with a continuous Lateral Orbital Sulcus (LOS, in blue). Type II, shown in the middle, is distinguished by continuity in both MOS and LOS. Type III, on the right, is characterized by a discontinuous MOS and discontinuous LOS. Orange line indicates Transverse Orbital Sulcus (TOS), and green line indicates Intermediate Orbital Sulcus (IOS), which are traced to assist in sulcus orientation and identification, but are not relevant to sulcogyral pattern type. (Note: The sample subjects included in this image were chosen with the same pattern type in both hemispheres for illustrative purposes. It is not typical for a subject to exhibit the same pattern type in both hemispheres.)

3.4.4 Voxel-Based Morphometry Gray Matter Analysis

In addition to identifying the sulcal pattern types, a VBM analysis was completed to investigate differences in GM volume in specific brain regions of the OFC between control and BP groups (Ashburner & Friston, 2000). FSL software was used to extract brain information, create a study-specific reference template using a random sample of 20 images (10 BP, 10 Control), process the population of 98 images, and obtain a quantification of gray matter volume. The Automated Anatomical Labeling 2 (AAL2) digital atlas of the human brain was used to identify segments of the OFC in a three-dimensional space (Rolls, Joliot, & Tzourio-Mazoyer, 2015). Masks for the overall left and right OFC, as well as medial, anterior, posterior, and lateral subregions were derived from regions 25-32 in AAL2 atlas. These masks were then used to obtain estimates of OFC GM, bilaterally. (All 98 subjects were included in this analysis; see Table 1a for details).

3.4.5 Diffusion Tensor Imaging

Diffusion tensor magnetic resonance imaging (DTI) analysis was employed to investigate long-range WM structural connectivity within the OFC. The DTI pipeline used in our tractography analysis was adopted from a workflow generously shared by the Olson Lab (Metoki, Alm, Wang, Ngo, & Olson, 2017). DTI data were coregistered to a T_1-weighted MPRAGE scan and aligned to the AC-PC plane. DW-MRI acquired from the publically available dataset were put through a processing pipeline in FSL following a

typical workflow, which included eddy current correction. The b-vector matrix was then

corrected for gross subject motion. A binary mask was then created in which the b-naught

image was extracted from the eddy-corrected DTI file. Using FSL BET, brains were

extracted and skull matter was stripped (Smith, 2002). Quality control checks were

implemented after each step to verify the mask's fit and accuracy of the brain extraction.

As described previously, several participants were excluded (N=15) in this analysis due

to excessive motion, missing DWI data, or an inappropriate angle of acquisition (see

Table 1b for demographic info regarding the subgroup used in DTI analysis). The

diffusion tensor variable was then created in FSL to fit the tensors to each voxel, yielding

a measure of fractional anisotropy (FA) extracted from the diffusion images.

Diffusion ToolKit software (Wang, Benner, Sorensen, & Wedeen, 2007) was used

to implement a 3D white matter reconstruction of the DWI images, which were viewed

and further analyzed in TrackVis software (Wang et al., 2007). On a subject-by-subject

basis, the FSL-preprocessed DTI image created for FA scalar/tensor was overlaid on the

3D white matter tract reconstruction in TrackVis. White matter tracts specific to the UF

were isolated bilaterally in each subject according to an objective, standardized protocol

(Metoki et al., 2017). UF tracts, which connect the temporal and frontal lobes of the brain

in a hook-shaped fashion, were isolated by placing regions of interest on the temporal and

frontal lobes of a slice of the coronal plane (Figure 2). This restricted the tract group to

only contain WM tracts crossing through the manually-positioned ROIs. Figure 2

provides an example UF region of tracts isolated with two ROIs. Once the UF was

isolated, statistical measures were exported using TrackVis software. These included

mean FA values and the number of tracts isolated within the UF.
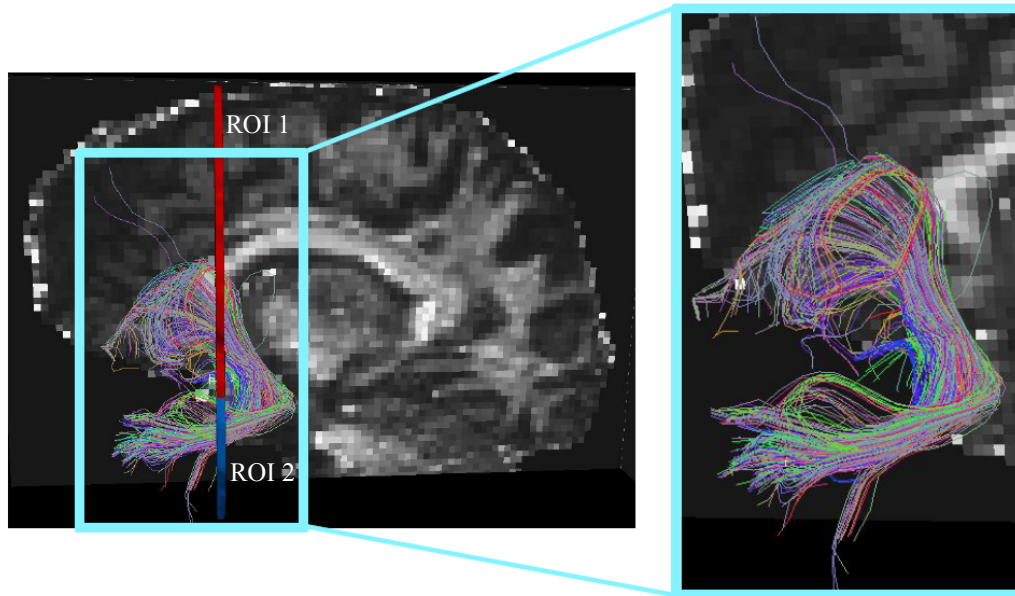
Figure 2. **Example tractography image of uncinate fasciculus (UF) in left**

hemisphere of sagittal plane in sample DW-MRI image. Regions of interest (ROI 1 in

red; ROI 2 in blue; shown in image on left) were placed in coronal planes of DW-MRI

white matter reconstructions in TrackVis software to isolate the UF. Image on the right

depicts a close-up of a typical hook-shaped bundle of UF tracts. Different colors in

images represent directionality of diffusion in the individual white matter tracts.

3.5 Statistical Analysis

Statistical analyses were performed using SPSS (IBM SPSS 23.0 for Mac, SPSS

Inc., Chicago, Illinois). We first assessed whether there were any demographic

differences across groups in gender ratio and scanner site using χ^2 statistics. Additionally,

we assessed whether there were any differences in the demographic variables of age or education across groups. In the case that this statistical test was significant between controls and BP, analysis was followed up with independent sample t-tests in order to compare groups to each other and establish which group differences were driving these effects. We also assessed whether there were any phenotypic differences between groups on quantitative psychometrics that are relevant to these populations. Similar to demographic analyses, we first assessed whether there were differences between groups. These comparisons were then followed-up with independent sample t-tests. Analyses of demographic and phenotypic differences were not part of the main hypothesis, but were completed in order to confirm that BP and controls were different from each other in expected ways. Inter-hemispheric distribution of OFC sulcogyral pattern types in the left and right hemisphere were established in patients and compared to controls using χ^2 statistics. Following these analyses, the specific pattern type (I, II, or III) which differentiates the groups was explored by comparing frequency distributions within one pattern relative to all other patterns (i.e. proportion of Type I vs. not Type I, proportion of Type II vs. not Type II, and so on) using χ^2 statistics. Analyses were then completed to confirm whether previously identified phenotypic differences are related to sulcogyral patterns.

Additionally, GM volumetric differences between controls and BP were assessed with one-tailed, type two independent sample t-tests. One-tailed t-tests were used here because we expected BP patients to display reductions in GM relative to controls. Statistics on FA measurements and the number of WM tracts in UF were analyzed using

two-tailed, independent sample t-tests to assess differences between controls and BP.

Two-tailed t-tests were employed because we had no specific expectations as to how the

tracts would differ in BP relative to controls (i.e., either increased or decreased). For all

analyses, p-values are reported, and values of $p<0.05$ are considered to be significant,

while values of $p<0.10$ are considered to be trending toward significance. These results

are not corrected for multiple comparisons.

4. Results

4.1 Demographic Differences

We assessed demographic differences between BP and HC subjects included in the sulcogyral pattern tracing and voxel-based morphometry analyses. Chi-squared analyses and independent t-tests comparing BP to HC (t(98)=-2.47, p=0.015) (see Table 1a) indicated that BP subjects were slightly older. However, OFC sulcogyral patterns are thought to be constant throughout life (Armstrong, Schleicher, Omran, Curtis, & Zilles, 1995), and thus, a slight age difference between our groups should not significantly impact the results. We then assessed differences in the distribution of male and female subjects within the groups with χ^2 statistics (χ^2(2, N=98)=2.04, p=0.153, NS). As mentioned earlier, subjects within the HC and BP groups were scanned on two scanners at separate sites. OFC sulcogyral pattern is a stable brain structure that should not be influenced by scanner site. Nonetheless, we used χ^2 statistics to assess the distribution of patients scanned on each scanner. This analysis revealed that the distribution of patients scanned on either scanner was significantly different (χ^2(2, N=98)=7.88, p=0.005) (Table 1a).

Upon excluding additional participants whose diffusion-weighted images did not pass our quality check (HC N=10, BP N=5), we again assessed demographic differences between the groups (HC N=42, BP N=41). We did not expect that the exclusion of participants would affect the demographic differences. Nonetheless, we employed χ^2 statistics to assess potential differences in the subgroup of participants in DTI analysis

(Table 1b). Chi-squared analyses and independent t-tests comparing the ages of BP to HC

(t(83)=-2.39, p=0.019) also indicated that BP subjects in the DTI subgroup were slightly

older. The distribution of male and female subjects remained insignificant (χ^2(2,

N=83)=1.49, p=0.222, NS). Additionally, the distribution of patients scanned on the two

scanner sites remained significantly different (χ^2(2, N=83)=4.63, p=0.031) (Table 1b).

4.2 Phenotypic Differences

Next we evaluated whether differences existed between the clinician-interview

and self-report instruments of all subjects between controls and BP with t-tests.

We compared scores on the self-report questionnaires acquired in all participants

to demonstrate differences between HC and BP groups (see Table 2, left panel). Scores

on HPS (t(98)= - 4.51, p<0.001) and Bipolar II Summary Score (BPII) (t(98)= - 5.37,

p<0.001) indicate significant differences between HC and BP groups.

The exclusion of subjects for the DTI subgroup was not expected to influence

phenotypic differences. Nonetheless, we compared scores on the self-report

questionnaires in the subgroup of participants included in the DTI analysis. Scores on

HPS (t(83)= - 4.29, p<0.001) and BPII (t(83)= - 4.92, p<0.001) indicate significant

differences between HC and BP groups.

4.3 Sulcal Pattern Types

Table 3 contains the number of subjects identified to have each sulcogyral pattern type, with a distinction between the left and right hemisphere. Results from χ^2 tests are depicted in Figure 3. Within the left hemisphere, overall pattern type frequency for BP differed significantly from the control group ($\chi^2(2, N=98)=18.6$, p<0.001). There was no significant difference in sulcogyral pattern frequency between patient groups in the right hemisphere ($\chi^2(2, N=98)=0.038$, p=0.981, NS).

We then assessed which specific pattern types differentiated the groups. This analysis was limited to the left hemisphere, since there was no indication that right hemisphere OFC pattern distributions differed between BP and controls. In the left hemisphere, BP exhibited a reduced Type I pattern frequency relative to controls ($\chi^2(2, N=98)=17.73$, p<0.001). There was no significant difference in Type II pattern expression between BP and controls ($\chi^2(2, N=98)=3.291$, p=0.070, NS). BP patients had increased prevalence of Type III patterns on the left hemispheres relative to controls ($\chi^2(2, N=98)=11.03$, p<0.001). Thus, differences in OFC sulcogyral pattern distributions between BP and controls are likely driven by decreased presence of Type I and increased presence of Type III in the BP group.

Table 3. **Sulcogyral pattern types in orbitofrontal cortex.**

	HC (N=52)		BP (N=46)		HC vs. BP χ^2 / F / t (p)
	N	**%**	**N**	**%**	
Left OFC Pattern					
Type I	41	79	17	37	18.6 (p<0.001)
Type II	7	14	13	28	
Type III/IV	4	8	16	35	
Right OFC Pattern					
Type I	31	60	28	60	0.038 (p=0.981)
Type II	10	19	9	20	
Type III/IV	11	21	9	20	

HC = healthy controls; BP = bipolar
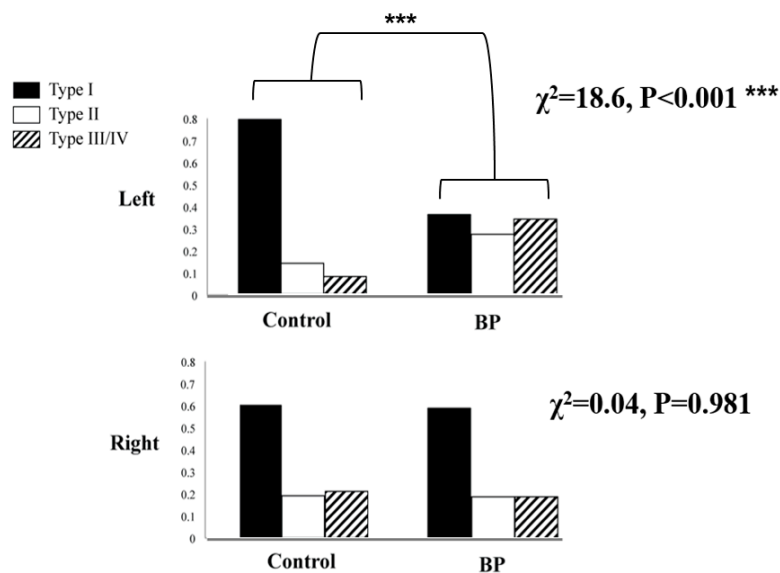
Figure 3. Chi-squared test results of OFC sulcogyral pattern type. Pattern

frequencies are shown for each Type, organized in columns according to subject group.

Frequencies of pattern type for each hemisphere of subject group add to a frequency of 1.

(BP = bipolar disorder).

4.4 Voxel-Based Morphometry Gray Matter Analysis

Using the AAL2 atlas, a VBM analysis was employed to assess GM volumetric

differences within the OFC. This was done for overall left and right OFC volume, as well

as within subregions defined in the atlas.

To assess GM differences within the entire OFC, left and right OFC masks were

created by combining medial, anterior, posterior, and lateral OFC subregion masks from

the AAL2 atlas (combining OFC regions 25-32 in the atlas). These were then used to

extract average GM volumes for the left and right OFC. T-tests indicated that BP patients exhibited reduced GM volume relative to controls in both the left (p=0.0039) and right (p=0.0338) hemispheres of the OFC.

Next, we extracted average GM volume for each subgregion of the OFC, bilaterally. T-tests with one-tailed distribution and two-sample equal variance were then employed to assess differences between estimates of GM volumes in BP and controls (see Figure 4, purple box).

No differences existed between the left (p=0.239) and right (p=0.175) hemispheres of the lateral OFC for controls and BP (Figure 4, blue box). Within the anterior OFC, GM volumes did not differ significantly between controls and BP in the right hemisphere (p=0.154). However, BP subjects exhibited decreased GM volume relative to controls within the left hemisphere of the anterior OFC (p=0.032) (Figure 4, teal box). Within the posterior subregion of the OFC, BP patients displayed reduced GM volume relative to control subjects in both the left (p=0.0046) and right (p=0.0414) hemispheres (Figure 4, yellow box). Lastly, within the medial OFC, BP subjects showed significantly reduced GM volume relative to controls (p=0.0122) in the left hemisphere, while there was a trend towards difference between BP and HC subjects' GM volumes in the right hemisphere (p=0.0582) (Figure 4, red box).

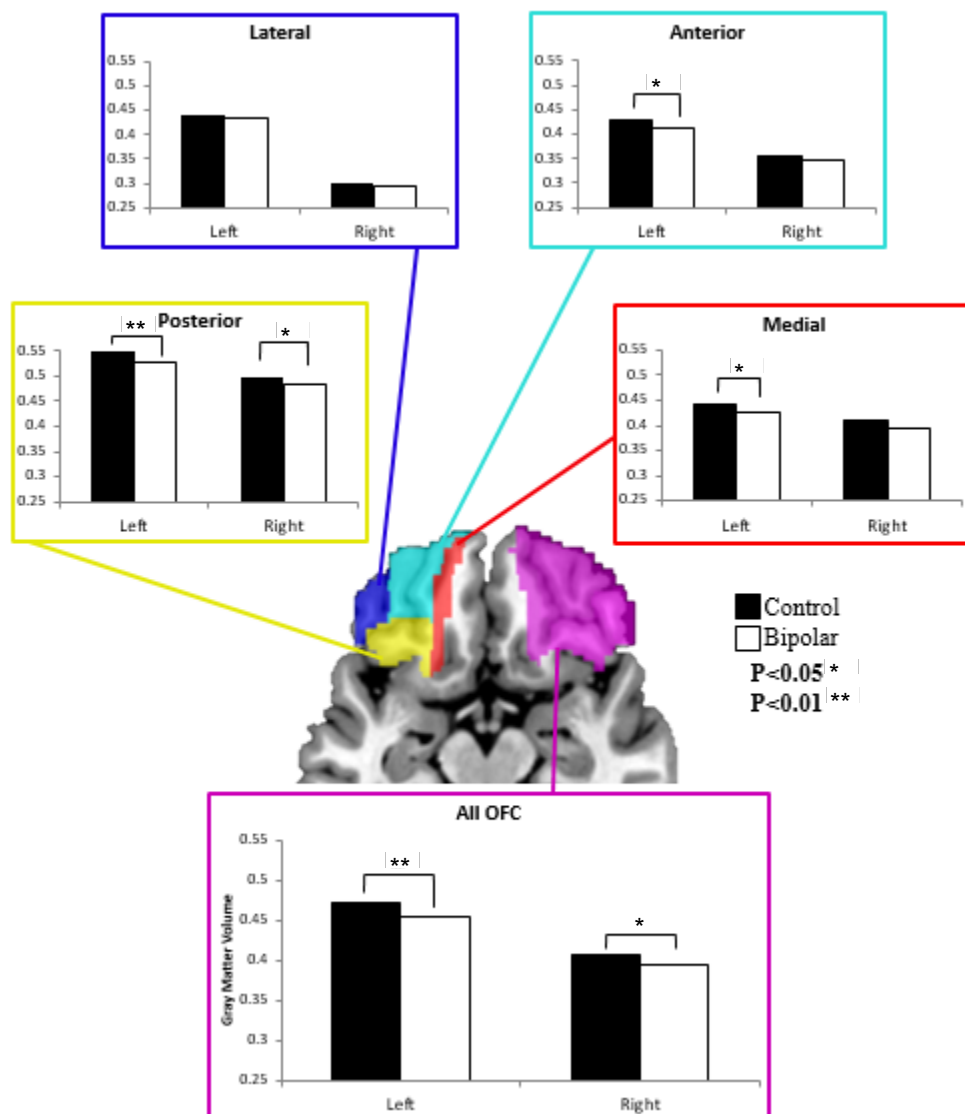**Figure 4. Gray matter volumetric differences in local and global OFC.** Each masked region on the sample brain image corresponds to a callout graph illustrating the gray matter volumes within that region in each hemisphere. Yellow represents posterior OFC, blue represents lateral OFC, teal indicates anterior OFC, and red signifies medial OFC. The purple region represents all OFC subregions for a global analysis. Black bars

represent control subjects, and white bars indicate bipolar disorder patients. Significance of $P<0.05$ is denoted by * and significance of $P<0.01$ is denoted by **.

4.5 Uncinate Fasciculus Measurements

DTI analysis isolating the white matter (WM) uncinate fasciculus (UF) tracts yielded measurements of mean fractional anisotropy (FA). When two-tailed independent, two-sample t-tests were employed, no significant differences were found between controls (0.352 ± 0.03) and BP (0.349 ± 0.04) mean FA in the left uncinate ($p = 0.772$). Similarly, no significant differences were found between mean FA of controls (0.346 ± 0.03) and BP (0.336 ± 0.04) in the right uncinate ($p = 0.163$) (Table 4).

In the interest of further quantifying structural properties of the UF in patients, we then assessed differences in the number of tracts contained in the UF of both hemispheres. Interestingly, in the left uncinate, BP patients exhibited a reduced number of tracts (110 ± 36) relative to HC (125 ± 40) trending toward significance ($p = 0.094$). No differences in number of tracts were found between HC (130 ± 47) and BP (125 ± 43) in the right uncinate ($p = 0.627$) (Table 4).

Table 4. Fractional anisotropy (FA) measurements of bilateral uncinate fasciculi (UF). Top rows indicate measurements collected from UF of left hemispheres of subjects, and bottom rows exhibit results from UF of right hemispheres. Fifteen subjects were excluded (HC N=10, BP N=5) prior to DTI analysis, yielding N=83 (HC N=42, BP N=41).

		HC *(N=42)*	**BP** *(N=41)*	HC vs. BP
Left Uncinate	Mean FA (SD)	0.352 (0.03)	0.349 (0.04)	$p = 0.772$
	Mean Number of Tracts (SD)	125 (40)	110 (36)	$p = 0.094$
Right Uncinate	Mean FA (SD)	0.346 (0.03)	0.336 (0.04)	$p = 0.163$
	Mean Number of Tracts (SD)	130 (47)	125 (43)	$p = 0.627$

HC = healthy controls; BP = bipolar

5. Discussion

5.1 OFC Sulcogyral Patterns

Prior work has associated atypical sulcogyral patterns (Type II and Type III/IV) within the H-sulcus to disorders such as schizophrenia. In an extension of our lab's previous work (Patti & Troiani, 2018), here we provide evidence that atypical OFC sulcogyral patterns may also be present in bipolar disorder. Recent genetic evidence has indicated similar underlying etiology for several disorders, including schizophrenia and bipolar disorder, amid other forms of developmental brain dysfunction (DBD). The DBD model suggests that brain dysfunction manifests in clinical disorders encompassing less severe disorders of minimal cerebral dysfunction (eg, learning disabilities, ADHD), classic neurodevelopmental disabilities (eg, autism spectrum disorders), and some traditional neuropsychiatric disorders (eg, SZ, major affective disorders) (Moreno-De-Luca et al., 2013). According to this framework, a considerable subset of neurodevelopmental and neuropsychiatric diagnoses share risk factors, and the cause of each disorder can result in a spectrum of impairment severity (Moreno-De-Luca et al., 2013).

Consistent with our original hypothesis, we find that sulcogyral pattern frequency differs in BP patients relative to controls, specifically in the left hemisphere. This hypothesis was based on the overlap in symptoms of bipolar disorder and schizophrenia

(Maier, Zobel, & Wagner, 2006) and similar underlying genetic etiology (Cardno & Owen, 2014; Jackson, Fanous, Chen, Kendler, & Chen, 2013; Lichtenstein et al., 2009).

The OFC has been implicated in "personality" and may be critical to cognitive skills that make us fundamentally human. Further, abnormalities within the OFC have been associated with a range of disorders (Jackowski et al., 2012). It could be that the OFC is implicated in disorders due to the complex nature of this cortical region. The OFC is divided into subregions that demonstrate distinct cellular architecture and connectivity (Carmichael & Price, 1996; Kahnt, Chang, Park, Heinzle, & Haynes, 2012). Given the dense interconnections between these cortical and subcortical structures, it is not surprising that deviations from typical cortical folding would lead to brain disorders. In the context of OFC sulcogyral pattern types, Type I pattern is expected to be the standard sulcogyral folding that denotes the ideal spatial arrangement for efficient communication between brain regions. Thus, abnormalities relative to the Type I pattern (Type II and Type III/IV) likely lead to suboptimal neuronal communication between brain regions, which may manifest as atypical cognitive and phenotypic traits, and/or brain disorders.

5.2 Gray Matter Analysis

Confirming our hypothesis, the VBM analysis yielded reduced GM volumes in overall OFC in BP relative to controls within the left hemisphere. Additionally, GM reductions in BP relative to controls were present in left anterior, left and right posterior, and left medial OFC subregions. This hypothesis was based on overlapping symptoms

between SZ and BP, as well as previous research that has revealed GM reductions in SZ (McIntosh et al., 2005) and bipolar patients (Frangou et al., 2005; Nugent et al., 2006). Consistent with previous findings, this result adds to the growing body of literature regarding GM in bipolar patients, specifically within the OFC.

Reduced GM volumes in the OFC is supported by a previous meta-analysis of ROI studies, which demonstrated that BP exhibited reduced GM volumes in the frontal cortex relative to controls (Arnone et al., 2009). Contemporary models suggest that mood dysregulation in BP is the result of frontolimbic abnormalities (Strakowski et al., 2005). Specifically, GM reductions in the anterior, posterior, and medial OFC subregions may be of functional significance regarding BP. Lesion studies in primates targeting the anterior OFC have suggested that the subregion contributes to the regulation of negative emotions, such as anxiety and fear responses (Agustín-Pavón et al., 2012). In addition, the medial portion of the OFC has been implicated in mood disorders such as depression, as damage to this subregion results in deficits in emotion, mood, and social regulation, but does not impact cognition (Damasio, Grabowski, Frank, Galaburda, & Damasio, 1994). Investigating OFC subregions might inform further hypotheses related to functional impairments of BP. Assessing structural abnormalities of OFC subregions might also contribute to a greater understanding of sulcogyral patterns, as the subregions overlap with orbitofrontal sulci.

5.3 Tractography

Partially consistent with our final hypothesis, we found that the average number of tracts within the left UF of bipolar patients was trending toward a significant reduction relative to controls. However, we did not find significant differences in mean FA measurements in either left or right hemispheres between BP and controls.

It is meaningful that the number of tracts within the UF was reduced in BP subjects relative to controls. White matter tracts are composed of myelinated axons which connect gray matter regions and carry nerve impulses between neurons. Thus, given the cognitive, behavioral, and emotional impairments associated with disorders such as bipolar disorder, it is unsurprising that less tracts exist in BP patients in the UF, which connects regions of the limbic system critical for emotion and behavior. Further tractography research isolating the UF should include the number of tracts in their investigations.

Our findings did not indicate any significant FA results within the UF of bipolar patients relative to controls. However, the literature demonstrates mixed findings on the UF properties of clinical populations relative to controls. Several findings indicate that BP exhibit decreased WM relative to controls (Adler et al., 2004; McIntosh et al., 2005; McIntosh et al., 2008; Regenold et al., 2006; Sussmann et al., 2009). However, other findings report no WM differences in prefrontal subregions (López-Larson, DelBello, Zimmerman, Schwiers, & Strakowski, 2002), no FA differences in bipolar UF (Houenou et al., 2007), and even increased UF fibers between the left subgenual cingulate and left

amygdalo-hippocampal regions (Houenou et al., 2007). Future research should seek to clarify the relevance of FA measurements and the specific WM deficits various clinical populations demonstrate.

5.4 Limitations and Future Directions

The information presented here is not without its limitations. Our results were not corrected for multiple comparisons. We should continue to accumulate a database of OFC sulcogyral characterizations in several diagnostic groups in order to obtain the power necessary to complete rigorous statistical testing with multiple comparison correction. Additionally, this study and other work demonstrate significant differences between control and patient groups on demographic variables, such as education level, in addition to atypical sulcogyral pattern frequencies. It has been shown that individuals with mental illness are less likely to pursue higher education relative to individuals without mental illness (Eaton et al., 2008). It can be difficult to determine whether differences in demographic variables are related to OFC sulcogyral pattern type given the close relationship between psychiatric illness and education. Future work might address whether educational attainment is associated with OFC sulcogyral pattern type.

VBM is a technique that has been used for nearly two decades to quantify gray matter differences between groups. The accuracy of VBM depends on precise image registration and normalization (McIntosh et al., 2005). Thus, this method of brain

analysis does not take into account large variations in brain structure that may be present in a more heterogeneous cohort.

The DTI pipeline implemented in the present study, though adopted from a standardized protocol used in a previous lab (Metoki et al., 2017), was novel to our lab. The protocol was performed according to established methods and implemented consistently for each subject. However, tractography analysis employed to isolate the UF in each subject is based on partially subjective classifications. That is, it was up to the independent individual performing tractography analysis to manually place regions of interest in the appropriate brain regions in each individual subject bilaterally to yield the UF tracts unique to each subject. Future work might aim to automate tractography analyses to identify white matter tracts such as the UF in an attempt to reduce any potential bias or manual error.

Additionally, it is worth noting that subjects within the BP group had exposure to various medications prior to and at the time of scanning. Although the OFC continues to develop following birth, the sulcal patterns are thought to be laid down during fetal development. Thus, it is unlikely that medication use would contribute to different OFC sulcogyral patterns in BP. Medication use could impact gray or white matter architecture and it is unclear how this might interact with sulcogyral pattern type. Future work should attempt to clarify the effects of medications on brain architecture and its relationship to quantitative measures of symptoms.

It might also be worth investigating the other subtypes of bipolar disorder. Our analysis and previous research on sulcogyral patterns has focused on Bipolar I, but it

would be interesting to assess the frequency distributions of sulcogyral pattern types in individuals with Bipolar II, Cyclothymia, and/or Bipolar, unspecified. In addition to sulcogyral patterns potentially being used to differentiate disorders, further investigation of sulcogyral patterns may provide a distinguishable marker between bipolar subtypes.

5.5 Concluding Remarks

Overall, we find that atypical sulcogyral OFC patterns are found at a higher frequency relative to controls within the left hemisphere of bipolar disorder, gray matter volumes in the left OFC are significantly reduced in bipolar patients relative to controls, and the amount of tracts comprising the UF is significantly smaller in the left UF of bipolar patients compared to controls. Interestingly, there is a consistent pattern of atypical structural properties specific to the left hemisphere. Exploring and quantifying various structural brain properties, specifically within the OFC, such as sulcogyral patterns, gray matter volumes, and white matter tracts, could be useful in assessing individual risk to disease or brain disorders. Ultimately, the combination of such structural properties might assist in a more personalized approach for diagnosis and treatment of brain dysfunction.

6. References

Adler, C. M., Holland, S. K., Schmithorst, V., Wilke, M., Weiss, K. L., Pan, H., & Strakowski, S. M. (2004). Abnormal frontal white matter tracts in bipolar disorder: a diffusion tensor imaging study. *Bipolar disorders*, *6*(3), 197-203.

Agustín-Pavón, C., Braesicke, K., Shiba, Y., Santangelo, A. M., Mikheenko, Y., Cockroft, G., ... & Roberts, A. C. (2012). Lesions of ventrolateral prefrontal or anterior orbitofrontal cortex in primates heighten negative emotion. *Biological psychiatry*, *72*(4), 266-272.

Alexander, A. L., Lee, J. E., Lazar, M., & Field, A. S. (2007). Diffusion tensor imaging of the brain. *Neurotherapeutics*, *4*(3), 316-329.

Alexander-Bloch, A., Giedd, J. N., & Bullmore, E. (2013). Imaging structural co-variance between human brain regions. *Nature Reviews Neuroscience*, *14*(5), 322.

Alm, K. H., Rolheiser, T., Mohamed, F. B., & Olson, I. R. (2015). Fronto-temporal white matter connectivity predicts reversal learning errors. *Frontiers in human neuroscience, 9.*

American Psychiatric Association. (2013). *Diagnostic and statistical manual of mental disorders* (5th ed.). Arlington, VA: American Psychiatric Publishing.

Armstrong, E., Schleicher, A., Omran, H., Curtis, M., & Zilles, K. (1995). The ontogeny of human gyrification. *Cerebral cortex*, *5*(1), 56-63.

Arnone, D., Cavanagh, J., Gerber, D., Lawrie, S. M., Ebmeier, K. P., & McIntosh, A. M. (2009). Magnetic resonance imaging studies in bipolar disorder and schizophrenia: meta-analysis. *The British Journal of Psychiatry*, *195*(3), 194-201.

Ashburner, J., & Friston, K. J. (2000). Voxel-based morphometry—the methods. *NeuroImage, 11*(6), 805-821.

Bartholomeusz, C. F., Whittle, S. L., Montague, A., Ansell, B., McGorry, P. D., Velakoulis, D., ... & Wood, S. J. (2013). Sulcogyral patterns and morphological abnormalities of the orbitofrontal cortex in psychosis. *Progress in Neuro-Psychopharmacology and Biological Psychiatry*, *44*, 168-177.

Beaulieu, C. (2002). The basis of anisotropic water diffusion in the nervous system–a technical review. *NMR in Biomedicine, 15*(7- 8), 435-455.

Bora, E., Fornito, A., Pantelis, C., & Yücel, M. (2012). Gray matter abnormalities in major depressive disorder: a meta-analysis of voxel based morphometry studies. *Journal of affective disorders, 138*(1), 9-18.

Buchsbaum, M. S., Schoenknecht, P., Torosjan, Y., Newmark, R., Chu, K. W., Mitelman, S., ... & Ahmed, S. (2006). Diffusion tensor imaging of frontal lobe white matter tracts in schizophrenia. *Annals of general psychiatry, 5*(1), 19.

Burns, J.J., Job, D., Bastin, M.E., Whalley, H., Macgillivray, T., Johnstone, E.C., & Lawrie, S.M. (2003). Structural disconnectivity in schizophrenia: a diffusion tensor magnetic resonance imaging study. *The British Journal of Psychiatry, 182*(5), 439-443.

Cardno, A. G., & Owen, M. J. (2014). Genetic relationships between schizophrenia, bipolar disorder, and schizoaffective disorder. *Schizophrenia bulletin, 40*(3), 504-515.

Carmichael, S. T., & Price, J. L. (1996). Connectional networks within the orbital and medial prefrontal cortex of macaque monkeys. *Journal of Comparative Neurology, 371*(2), 179-207.

Carroll, L. S., & Owen, M. J. (2009). Genetic overlap between autism, schizophrenia and bipolar disorder. *Genome medicine, 1*(10), 102.

Chakirova, G., Welch, K. A., Moorhead, T. W. J., Stanfield, A. C., Hall, J., Skehel, P., ... & McIntosh, A. M. (2010). Orbitofrontal morphology in people at high risk of developing schizophrenia. *European Psychiatry, 25*(6), 366-372.

Chiavaras, M. M., & Petrides, M. (2000). Orbitofrontal sulci of the human and macaque monkey brain. *Journal of Comparative Neurology, 422*(1), 35-54.

Chye, Y., Solowij, N., Ganella, E. P., Suo, C., Yücel, M., Batalla, A., ... & Bartholomeusz, C. F. (2017). Role of orbitofrontal sulcogyral pattern on lifetime cannabis use and depressive symptoms. *Progress in Neuro-Psychopharmacology and Biological Psychiatry, 79*, 392-400.

Damasio, H., Grabowski, T., Frank, R., Galaburda, A. M., & Damasio, A. R. (1994). The return of Phineas Gage: clues about the brain from the skull of a famous patient. *Science, 264*(5162), 1102-1105.

Eaton, W. W., Martins, S. S., Nestadt, G., Bienvenu, O. J., Clarke, D., & Alexandre, P. (2008). The burden of mental disorders. *Epidemiologic reviews*, *30*(1), 1-14.

Eckblad, M., & Chapman, L. J. (1986). Development and validation of a scale for hypomanic personality. *Journal of abnormal psychology*, *95*(3), 214.

Fields, R. D. (2008). White matter in learning, cognition and psychiatric disorders. *Trends in neurosciences*, *31*(7), 361-370.

First, M.B., Spitzer, R.L., Gibbon, M., Williams, J.B. (1995) Structured Clinical Interview for DSM-IV Axis I Disorders-Patient Edition (SCID-I/P, Version 2.0).

Frangou, S., Donaldson, S., Hadjulis, M., Landau, S., & Goldstein, L. H. (2005). The Maudsley Bipolar Disorder Project: executive dysfunction in bipolar disorder I and its clinical correlates. *Biological Psychiatry*, *58*(11), 859-864.

Friston, K. J., & Frith, C. D. (1995). Schizophrenia: a disconnection syndrome. *Clinical Neuroscience*, *3*(2), 89-97.

Good, C. D., Johnsrude, I. S., Ashburner, J., Henson, R. N., Friston, K. J., & Frackowiak, R. S. (2001). A voxel-based morphometric study of ageing in 465 normal adult human brains. *Neuroimage*, *14*(1), 21-36.

Greve, D. N., & Fischl, B. (2009). Accurate and robust brain image alignment using boundary-based registration. *Neuroimage*, *48*(1), 63-72.

Houenou, J., Wessa, M., Douaud, G., Leboyer, M., Chanraud, S., Perrin, M., ... & Paillere-Martinot, M. L. (2007). Increased white matter connectivity in euthymic bipolar patients: diffusion tensor tractography between the subgenual cingulate and the amygdalo-hippocampal complex. *Molecular psychiatry*, *12*(11), 1001.

Jackowski, A.P., de Araújo Filho, G. M., de Almeida, A. G., de Araújo, C. M., Reis, M., Nery, F., … & Lacerda, A. L. (2012). The involvement of the orbitofrontal cortex in psychiatric disorders: an update of neuroimaging findings. *Revista Brasileira de Psiquiatria, 34*(2), 207-212.

Jackson, K. J., Fanous, A. H., Chen, J., Kendler, K. S., & Chen, X. (2013). Variants in the 15q25 gene cluster are associated with risk for schizophrenia and bipolar disorder. *Psychiatric genetics*, *23*(1), 20.

Jenkinson, M., Bannister, P., Brady, M., & Smith, S. (2002). Improved optimization for the robust and accurate linear registration and motion correction of brain images. *Neuroimage*, *17*(2), 825-841.

Jenkinson, M., & Smith, S. (2001). A global optimisation method for robust affine registration of brain images. *Medical image analysis*, *5*(2), 143-156.

Job, D. E., Whalley, H. C., McConnell, S., Glabus, M., Johnstone, E. C., & Lawrie, S. M. (2002). Structural gray matter differences between first-episode schizophrenics and normal controls using voxel-based morphometry. *Neuroimage*, *17*(2), 880-889.

Johansen-Berg, H. (2010). Behavioural relevance of variation in white matter microstructure. *Current opinion in neurology*, *23*(4), 351-358.

Kahnt, T., Chang, L. J., Park, S. Q., Heinzle, J., & Haynes, J. D. (2012). Connectivity-based parcellation of the human orbitofrontal cortex. *Journal of Neuroscience*, *32*(18), 6240-6250.

Kanai, R., & Rees, G. (2011). The structural basis of inter-individual differences in human behaviour and cognition. *Nature Reviews Neuroscience*, *12*(4), 231.

Kringelbach, M. L. (2005). The human orbitofrontal cortex: linking reward to hedonic experience. *Nature Reviews Neuroscience*, *6*(9), 691-702.

Kubicki, M., Westin, C. F., Maier, S. E., Frumin, M., Nestor, P. G., Salisbury, D. F., ... & Shenton, M. E. (2002). Uncinate fasciculus findings in schizophrenia: a magnetic resonance diffusion tensor imaging study. *American Journal of Psychiatry*, *159*(5), 813-820.

Lichtenstein, P., Yip, B. H., Björk, C., Pawitan, Y., Cannon, T. D., Sullivan, P. F., & Hultman, C. M. (2009). Common genetic determinants of schizophrenia and bipolar disorder in Swedish families: a population-based study. *The Lancet*, *373*(9659), 234-239.

Lavoie, S., Bartholomeusz, C. F., Nelson, B., Lin, A., McGorry, P. D., Velakoulis, D., ... & Wood, S. J. (2014). Sulcogyral pattern and sulcal count of the orbitofrontal cortex in individuals at ultra high risk for psychosis. *Schizophrenia research*, *154*(1), 93-99.

López-Larson, M. P., DelBello, M. P., Zimmerman, M. E., Schwiers, M. L., & Strakowski, S. M. (2002). Regional prefrontal gray and white matter abnormalities in bipolar disorder. *Biological Psychiatry*, *52*(2), 93-100.

Maier, W., Zobel, A., & Wagner, M. (2006). Schizophrenia and bipolar disorder: differences and overlaps. *Current Opinion in Psychiatry*, *19*(2), 165-170.

McIntosh, A. M., Job, D. E., Moorhead, T. W. J., Harrison, L. K., Forrester, K., Lawrie, S. M., & Johnstone, E. C. (2005). Voxel-based morphometry of patients with schizophrenia or bipolar disorder and their unaffected relatives. *Biological psychiatry*, *56*(8), 544-552.

McIntosh, A. M., Maniega, S. M., Lymer, G. K. S., McKirdy, J., Hall, J., Sussmann, J. E., ... & Lawrie, S. M. (2008). White matter tractography in bipolar disorder and schizophrenia. *Biological psychiatry*, *64*(12), 1088-1092.

Metoki, A., Alm, K. H., Wang, Y., Ngo, C. T., & Olson, I. R. (2017). Never forget a name: white matter connectivity predicts person memory. *Brain Structure and Function*, *222*(9), 4187-4201.

Monkul, E. S., Malhi, G. S., & Soares, J. C. (2005). Anatomical MRI abnormalities in bipolar disorder: do they exist and do they progress?. *Australian & New Zealand Journal of Psychiatry*, *39*(4), 222-226.

Moreno-De-Luca, A., Myers, S. M., Challman, T. D., Moreno-De-Luca, D., Evans, D. W., & Ledbetter, D. H. (2013). Developmental brain dysfunction: revival and expansion of old concepts based on new genetic evidence. *The Lancet Neurology*, *12*(4), 406-414.

Murray, E. A., O'Doherty, J. P., & Schoenbaum, G. (2007). What we know and do not know about the functions of the orbitofrontal cortex after 20 years of cross-species studies. *Journal of Neuroscience*, *27*(31), 8166-8169.

Nakamura, M., Nestor, P. G., Levitt, J. J., Cohen, A. S., Kawashima, T., Shenton, M. E., & McCarley, R. W. (2007a). Orbitofrontal volume deficit in schizophrenia and thought disorder. *Brain*, *131*(1), 180-195.

Nakamura, M., Nestor, P. G., McCarley, R. W., Levitt, J. J., Hsu, L., Kawashima, T., ... & Shenton, M. E. (2007b). Altered orbitofrontal sulcogyral pattern in schizophrenia. *Brain*, *130*(3), 693-707.

Nery, F. G., Chen, H. H., Hatch, J. P., Nicoletti, M. A., Brambilla, P., Sassi, R. B., ... & Soares, J. C. (2009). Orbitofrontal cortex gray matter volumes in bipolar disorder patients: a region- of- interest MRI study. *Bipolar disorders*, *11*(2), 145-153.

Nugent, A. C., Milham, M. P., Bain, E. E., Mah, L., Cannon, D. M., Marrett, S., ... & Drevets, W. C. (2006). Cortical abnormalities in bipolar disorder investigated with MRI and voxel-based morphometry. *Neuroimage*, *30*(2), 485-497.

Patti, M. A., & Troiani, V. (2018). Orbitofrontal sulcogyral morphology is a transdiagnostic indicator of brain dysfunction. *Neuroimage: Clinical*, *17*, 910-917.

Phillips, M. L., & Kupfer, D. J. (2013). Bipolar disorder diagnosis: challenges and future directions. *The Lancet*, *381*(9878), 1663-1671.

Price, G., Cercignani, M., Parker, G. J., Altmann, D. R., Barnes, T. R., Barker, G. J., ... & Ron, M. A. (2008). White matter tracts in first-episode psychosis: a DTI tractography study of the uncinate fasciculus. *Neuroimage*, *39*(3), 949-955.

Regenold, W. T., D'agostino, C. A., Ramesh, N., Hasnain, M., Roys, S., & Gullapalli, R. P. (2006). Diffusion- weighted magnetic resonance imaging of white matter in bipolar disorder: a pilot study. *Bipolar Disorders*, *8*(2), 188-195.

Rolls, E. T., Joliot, M., & Tzourio-Mazoyer, N. (2015). Implementation of a new parcellation of the orbitofrontal cortex in the automated anatomical labeling atlas. *Neuroimage, 122,* 1-5.

Skudlarski, P., Jagannathan, K., Calhoun, V. D., Hampson, M., Skudlarska, B. A., & Pearlson, G. (2008). Measuring brain connectivity: diffusion tensor imaging validates resting state temporal correlations. *Neuroimage*, *43*(3), 554-561.

Smith, S. M. (2002). Fast robust automated brain extraction. *Human brain mapping*, *17*(3), 143-155.

Strakowski, S. M., Delbello, M. P., & Adler, C. M. (2005). The functional neuroanatomy of bipolar disorder: a review of neuroimaging findings. *Molecular psychiatry*, *10*(1), 105-116.

Sussmann, J. E., Lymer, G. K. S., McKirdy, J., Moorhead, T. W. J., Maniega, S. M., Job, D., ... & McIntosh, A. M. (2009). White matter abnormalities in bipolar disorder and schizophrenia detected using diffusion tensor magnetic resonance imaging. *Bipolar disorders*, *11*(1), 11-18.

Takayanagi, Y., Takahashi, T., Orikabe, L., Masuda, N., Mozue, Y., Nakamura, K., ... & Kasai, K. (2010). Volume reduction and altered sulco-gyral pattern of the orbitofrontal cortex in first-episode schizophrenia. *Schizophrenia research*, *121*(1), 55-65.

Wang, R., Benner, T., Sorensen, A. G., & Wedeen, V. J. (2007, May). Diffusion toolkit: a software package for diffusion imaging data processing and tractography. In *Proc Intl Soc Mag Reson Med* (Vol. 15, No. 3720).

Wright, I. C., Rabe-Hesketh, S., Woodruff, P. W., David, A. S., Murray, R. M., & Bullmore, E. T. (2000). Meta-analysis of regional brain volumes in schizophrenia. *American Journal of Psychiatry*, *157*(1), 16-25.

Young, R. C., Biggs, J. T., Ziegler, V. E., & Meyer, D. A. (1978). A rating scale for mania: reliability, validity and sensitivity. *The British Journal of Psychiatry*, *133*(5), 429-435.

Yushkevich, P. A., Piven, J., Hazlett, H. C., Smith, R. G., Ho, S., Gee, J. C., & Gerig, G. (2006). User-guided 3D active contour segmentation of anatomical structures: significantly improved efficiency and reliability. *Neuroimage*, *31*(3), 1116-1128.